

H. Haker · H. Misslisch · M. Ott · M. A. Frens
V. Henn · K. Hess · P. S. Sándor

Three-dimensional vestibular eye and head reflexes of the chameleon: characteristics of gain and phase and effects of eye position on orientation of ocular rotation axes during stimulation in yaw direction

Received: 16 September 2002 / Revised: 3 April 2003 / Accepted: 12 April 2003 / Published online: 29 May 2003
© Springer-Verlag 2003

Abstract We investigated gaze-stabilizing reflexes in the chameleon using the three-dimensional search-coil technique. Animals were rotated sinusoidally around an earth-vertical axis under head-fixed and head-free conditions, in the dark and in the light. Gain, phase and the influence of eye position on vestibulo-ocular reflex rotation axes were studied. During head-restrained stimulation in the dark, vestibulo-ocular reflex gaze gains were low (0.1–0.3) and phase lead decreased with increasing frequencies (from 100° at 0.04 Hz to < 30° at 1 Hz). Gaze gains were larger during stimulation in the light (0.1–0.8) with a smaller phase lead (< 30°) and were close to unity during the head-free conditions (around 0.6 in the dark, around 0.8 in the light) with small phase leads. These results confirm earlier findings that chameleons have a low vestibulo-ocular reflex gain during head-fixed conditions and stimulation in the dark and higher gains during head-free stimulation in the light. Vestibulo-ocular reflex eye rotation axes were roughly aligned with the head's rotation axis and did not systematically tilt when the animals were looking eccentrically, up- or downward (as predicted by Listing's Law). Therefore, vestibulo-ocular reflex responses in the chameleon follow a strategy, which optimally stabilizes

the entire retinal images, a result previously found in non-human primates.

Keywords Chameleon · Dual search coil technique · Eye position dependence · Listing's law · Vestibulo-ocular reflex

Abbreviations 2D: two dimensional · 3D: three dimensional · LED: light emitting diode · LL: Listing's Law · OCR: opto-collic reflex · OKR: opto-kinetic reflex · VCR: vestibulo-collic reflex · VOR: vestibulo-ocular reflex · VP: velocity plane

Introduction

The chameleon is a lateral-eyed arboreal lizard that moves its eyes independently over a large range of 180° horizontally and 90° vertically (Sándor et al. 2001). Similar to primates chameleons have foveate eyes (Ott 1997; Pettigrew et al. 1999) and fixate objects of interest with saccadic eye movements. During binocular fixation of a prey, the visual fields overlap and both eyes converge. To prevent blurring of vision during movements of the animal's head, the gaze needs to be continuously stabilized by the vestibular and optokinetic reflexes. Perfect retinal image stabilization requires an eye-in-head rotation with the eye rotating, compared to the head's horizontal rotation examined in the present study in the opposite direction about a parallel (vertical) axis, and with equal velocity. The reflex response during sinusoidal stimulation can be characterized by the gain and the phase shift of the eye velocity signal compared to the stimulus signal. For optimal retinal image stabilization, with the head rotating horizontally, one would expect a gain of 1, a phase shift of 0 and vestibulo-ocular reflex (VOR) eye rotation axes that remain vertical although eyes actually look in various vertical directions. The latter finding would indicate that the VOR stabilizes the entire retinal image whether the animal looks up, down or straight ahead. This means

Volker Henn died on 3 December 1997

H. Haker (✉) · H. Misslisch · V. Henn · K. Hess · P. S. Sándor
Neurology Department, University Hospital of Zürich,
8091 Zürich, Switzerland

M. Ott
Department of Anatomy, University of Tübingen,
72074 Tübingen, Germany

M. A. Frens
Department of Neuroscience, ErasmusMC,
3000 DR Rotterdam, The Netherlands

H. Haker
Psychiatry University Hospital of Zürich, Lenggstrasse 31,
8029 Zürich, Switzerland
E-mail: haker@bli.unizh.ch
Tel.: +41-1-3842357
Fax: +41-1-3834456

that different eye positions require the programming of different muscle activations in order to generate the optimal response. The large oculomotor range of the chameleon makes it an ideal animal to study such processes. Stabilizing gaze reflexes of vestibular origin (VOR; and vestibulo-collic reflex, VCR) have been investigated previously in the chameleon using two-dimensional (2D) eye movement recordings (Gioanni et al. 1993, Kirmse 1988, Tauber and Atkin 1967). The VCR and OCR are compensatory reflexes of the neck. The VCR input comes from the vestibular system, the OCR input from the visual system. The characteristics of gain and phase of the head and gaze stabilizing reflexes have been described by Gioanni et al. (1993) for horizontal and vertical movements. To our knowledge our work is the first study characterizing gaze stabilization reflexes in the chameleon in all three rotational degrees of freedom and includes the effect of eye position on ocular rotation axes.

One goal of our study was to analyze the characteristics of gain and phase of the horizontal (yaw) VOR during different sinusoidal stimulation conditions (dark versus light, head-fixed versus head-free). A second goal of the study was to analyze the effect of eye (vertical) position on the horizontal VOR, allowing to compare strategies for retinal image stabilization between chameleons and primates (Misslisch et al. 1994). When examining the horizontal VOR of rhesus monkeys, Misslisch and Hess (2000) found that the eye rotation axes remained vertical, aligned with the head rotation axis, independent of the eyes' vertical positions. That is, the monkey's horizontal VOR optimally stabilizes the entire retinal image during horizontal vestibular stimulation in the light (the same holds for the monkey's pitch VOR when eye positions vary horizontally as well as for the roll VOR when eye positions change vertically and/or horizontally, see Misslisch and Hess 2000). In humans, however, the horizontal VOR's rotation axis changes systematically when gaze changes from one direction to another: the eye rotation axis is aligned with the axis of head rotation when the eye looks straight ahead; the eye rotation axis tilts upward when the eye is looking up; and the eye rotation axis tilts downward when the eye is looking down (Misslisch et al. 1994, Palla et al. 1999, Solomon et al. 1997). Quantitatively, the VOR eye rotation axis in humans tilts about a quarter as far as the gaze line (quarter-angle rule). What does that pattern mean functionally? To understand this, it is important to describe Listing's law (LL), a kinematic constraint that has been shown to be followed by eye movements such as saccades (Tweed and Vilis 1990) or smooth pursuit (Haslwanter et al. 1991; Tweed et al. 1992). Generally, LL predicts that for any eye position, the eye velocity vector must lie in a head-fixed plane (velocity plane, VP). This plane is fronto-parallel if we assume that the eye is in primary position (corresponding, in humans, to a position when the eye is looking approximately straight ahead, in chameleons, corresponding to a position when, for example, the right

eye is looking straight to the right). During horizontal head rotation, with the eye in this position, a VOR perfectly following LL rotates the eye around the vertical (head rotation) axis (which lies in the VP of primary position). But if the eye is looking, say 20° up, LL predicts that the VP tilts upward, relative to its orientation when the eye is in primary position; and if the eye is looking 20° down, the VP tilts downward. Quantitatively, LL implies VP tilts that correspond to half the change in gaze direction (half-angle-rule; see for example Tweed and Vilis 1990 or Misslisch et al. 1994). But if, as in our example, the chameleon looks 20° up or down, the VP tilt 10° up or down, the VOR's rotation axis, which was vertical when the eye was in the first position, has to tilt 10° up or down, when the VOR follows LL. Thus, if the VOR follows LL, the eye rotation axis has to tilt away from alignment with the invariantly vertical head rotation axis.

The human VOR pattern (quarter-angle rule) therefore resembles a compromise strategy between perfect retinal image stabilization (no tilt of the eye's rotation axis) on the one hand and compliance with LL (tilt according to the half-angle rule) on the other hand.

As an evolutionary old animal with a huge oculomotor range, the chameleon is an interesting subject to study the importance of the two different strategies, i.e., Listing's Law or the strategy of optimal retinal image stabilization.

Materials and methods

Animals

Experiments were performed on three chameleons: two animals of the species *Furcifer pardalis* (Ve and Pu) and one animal of the species *Chameleo oustaleti* (Mo).

Setup

Eye and head position recording

We measured three-dimensional (3D) eye and head position in a laboratory environment with the magnetic search coil technique using a 3-field system (Rommel system, modified by A. Lasker; for details see Straumann et al. 1995). To obtain miniature dual search-coils for 3D movement measurements, two coils (Sokimat, Switzerland, outer diameter 2 mm, weight 2.7 mg) were aligned orthogonally to each other and stabilized by crazy glue (3M, Switzerland). The diameter of the coil assembly was 2.5 mm, its weight about 7 mg.

The 3D eye position was recorded with a dual search-coil that was glued to the eyelid at the point of its anatomical fusion with the sclera, according to Sándor et al. (2001). Head position was recorded with a dual search coil glued to the animal's bony forehead. Both head and eye coils were removed after each experiment. Head-fixed conditions were performed using a custom-made, foam-padded head-frame and a body-holder to keep the head stationary with respect to coil frame and turntable. For the head-free recordings the animal was not restricted in its movements.

The animal was placed inside an aluminum cubic coil frame on a horizontal Plexiglas perch, to which it was holding on, using its

Table 1 Overview of stimulation conditions, including studied frequencies and peak velocities

Stimulation	Frequencies (Hz)	Peak velocities ($^{\circ} \text{ s}^{-1}$)
1. Vestibular, dark, head fixed	0.04–1.0	3–120
2. Vestibular, light, head fixed	0.04–1.0	15–120
3. Vestibular, dark, head free	0.2–1.0	3–40
4. Vestibular, light, head free	0.2–1.0	3–40

limbs and tail. The coil frame (side length 77 cm) itself was mounted on a servo-motor-driven turntable (diameter 120 cm). During all experimental conditions, the animals remained within the homogenous range of the magnetic field of the recording system.

Eye- and head-coil signals, as well as the turntable position, were sampled at a frequency of 1000 Hz per channel using a Pentium PC. The data were stored on hard disk for off-line analysis.

Vestibular and optokinetic stimulation protocols

Vestibular stimulation was carried out in complete darkness (vestibular only, to avoid possible fixation targets, any source of light was carefully covered, e.g., LEDs were taped) and in the presence of a stationary visual surround (combined vestibular and visual stimulus).

The animal's level of alertness was checked visually during the rests between the single stimulations. If needed, the animal was woken acoustically.

We tested the ocular stabilization reflexes using sinusoidal stimulation about the vertical axis (=horizontal, or yaw, VOR) with different frequencies and peak-velocities (Table 1), with at least 2 min of rest between different stimulation conditions. The stimulation conditions for the tested reflexes and their combinations were the following: (1) vestibular stimulation in the dark with the head restrained; (2) vestibular stimulation in the presence of a stationary visual surround with the head restrained; (3) vestibular stimulation in the dark with the head freely moving; and (4) vestibular stimulation with a stationary visual surround and the head freely moving.

Calibration and data representation

To determine dual search-coil sensitivities, in vitro calibration of the coil system was done according to Straumann et al. (1995). In brief, voltage offsets were nulled by connecting the search coils to the detector and then placing them in a metal tube that shielded the magnetic fields. Gains of the three magnetic fields were determined by mounting the connected dual search coil on a gimbal and recording maximal induced voltages in each field. For in vivo calibration, the experimenter observed the corneal reflection of a torch in the chameleon's eye through a pinhole to obtain a reference position with respect to the coil frame. The position of this pinhole was fixed in space and positioned in the reference direction that corresponded to the center of the oculomotor range. Eye positions were marked in the data file when the corneal reflex appeared in the middle of the pupil at least five times consecutively. Reference position was defined as the mean of the marked eye positions. This allowed determining eye in space position with an accuracy of 2° visual angle.

The 3D eye positions were represented as rotation vectors (Haustein 1989). In this description, every eye position is a 3D vector. The reference position for the eye was defined by in vivo calibration as described above. The direction of the vector is given by the direction of the rotation axis from the reference position to the current eye position. Vector length is $\tan(\alpha/2)$, with α being the angle of rotation.

Eye positions were expressed relative to orthogonal and right-handed field coordinates. The x , y , and z components corresponded to torsional, vertical, and horizontal eye positions, respectively. According to conventions the lateral-eyed chameleon was oriented with its snout in positive y -direction, therefore looking in positive x -direction with its right eye (Sándor et al. 2001). Positive rotation directions for the right eye were extorsion, down and left, accordingly to the right hand rule. For convenience, values were converted to degrees. As we used a reference position roughly in the middle of the oculomotor range of about 180° , the obtained values were maximum about $\alpha = \pm 90^{\circ}$, which can be dealt with using rotation vectors. As the reference frame was fixed with respect to the turntable, this was also true during stimulation.

Data analysis

Eye and head movement data were recorded in magnetic field coordinates. During vestibular stimulation, the coil frame was rotating with the turntable. Rotation vectors of the eye and head movement were further processed using MATLAB, version 5.1. Data files recorded under head-restrained conditions, where small attempted head movements in spite of the head holder occurred (controlled by the 2D search coil), were not analyzed. For analyzing the slow phase eye velocity, digitized 3D eye and head position data were desaccaded with a semiautomatic computer program. (Megadet, by Paul Hofman)

Analysis of horizontal gain and phase of the vestibular and optokinetic reflexes

A sinusoidal function was fitted to the turntable- and the desaccaded horizontal eye velocity signal over periods of at least two successive cycles. The gain was computed as peak slow phase velocity divided by peak stimulation velocity, phase shift as phase of the response signal minus phase of the stimulus signal. For the head-free conditions, a sinusoidal function was also fitted to the horizontal head velocity signal, and the gain and phase difference of the head signal were calculated. Correlations were performed using Spearman rank order correlations with $P < 0.05$ considered as statistically significant.

Analysis of the position-dependence of the VOR

The 3D input-output properties of the VOR can be quantified by computing the eye (e) and head (h) velocity vectors (each with torsional, vertical and horizontal components) during rotations about various axes and then computing the 3×3 matrix G such that the matrix-vector product Gh was the best possible approximation to e . Such an analysis has been performed to study the human horizontal, vertical and torsional VOR (Tweed et al. 1994a, 1994b). In a similar way, one can measure e , h and eye position (p) and compute (by the method of least-squares fitting) a best fit function relating them:

$$e = s + Gh + BhP, \quad (1)$$

where s is a three-component vector representing spontaneous nystagmus (ocular drift); G is a 3×3 matrix which acts on the vector h to yield a vector Gh ; and B is a 3×3 array of numbers, which acts on the two vectors h and p to yield a vector Bhp . This equation has been named the generalized gain function in studies on the influence of eye position on the human (Misslisch et al. 1994) and monkey (Misslisch and Hess 2000) horizontal, vertical and torsional VOR. In the present study, we used a similar technique, although we measured eye velocity only in response to horizontal head rotations (i.e., in the matrix, the input vectors for vertical and torsional head velocity were set to zero; hence, the products between torsional and vertical head velocity and the three components of eye positions yielded zero values for the respective elements in the generalized gain matrix).

Counting all the components in s , G and B , yields a $3 + 9 + 27 = 39$ -parameter description of the VOR, which characterizes the relationship of head velocity and eye position in determining VOR eye velocity. Now, tables showing the 39 parameters of the generalized gain matrix are difficult to interpret. Thus, we chose a different technique, which allows the unpacking of the information in these numbers: having computed the generalized gain matrix e , G and B , we input a vector h , representing some head velocity, and a vector p , representing some eye position, into Eq. 1 to yield the eye velocity evoked by that head velocity (in our study horizontal head velocity) when the eye is in that position. We then used different values of p (vertical eye position center and 20° up and 20° down), and calculated the corresponding eye velocity responses to expose whether the chameleon yaw VOR was influenced by eye position.

To obtain valid results for eccentric eye positions, we selected the files by the size of the performed oculomotor range. A broad exploration over a large part of the oculomotor range was only present during stimulation in the light. For reasons of signal-to-noise-ratio, the analytic technique can only be applied for data with a large oculomotor range and also with relative large eye velocities. As this was only the case during vestibular stimulation in the light, for this analysis we focused on two peak head velocities (20 and 40° s^{-1}) with a mean vertical oculomotor range greater than 70° . Since the applied analytical approach is only valid for data with small phase shift between the stimulus and the eye position signal, only files with a phase difference smaller than 7° were analyzed.

According to Misslisch et al. (1994), we describe the orientation of the slow phase rotation axes by a tilt angle relative to the orientation of the slow phase rotation axis during center gaze (typically close to vertical). Only the relative tilt angles were defined as positive when the eye's rotation axis for eccentric eye position tilted in the direction of gaze (negative vertical direction for upward gaze, positive vertical direction for downward gaze), as predicted by Listing's law.

Results

Response characteristics of gain and phase of the vestibular and optokinetic reflexes

Head-restrained condition

In the absence of a visual surround the vestibulo-ocular reflex gains were relatively small, ranging from 0.01 up to about 0.5 . Overall, there was a minimal increase of gain with increasing stimulation frequency (Fig. 1A). In one animal (Ve), gains decreased from about 0.5 to 0.1 with increasing stimulation velocities, while in the other two animals small gains were found (0.1 – 0.2) with a similar, but much smaller decrease (Fig. 1B). The phase difference was maximal for low frequencies with a phase lead of around 90° in two animals (Ve, Pu) and around 120° in the third animal (Mo), decreasing towards smaller values of around zero (Ve) or 30° (Pu, Mo) with increasing stimulation frequencies (Fig. 1C).

Combined visual-vestibular stimulation (Fig. 2) resulted in mean gains of about twice the magnitude compared to pure vestibular responses. Again, one animal (Ve, mean gain 0.4) showed higher gains as the two others (Pu, Mo, mean gain 0.25), although with similar characteristics. The gain did not show any significant dependence on stimulation frequency (Fig. 2A), but

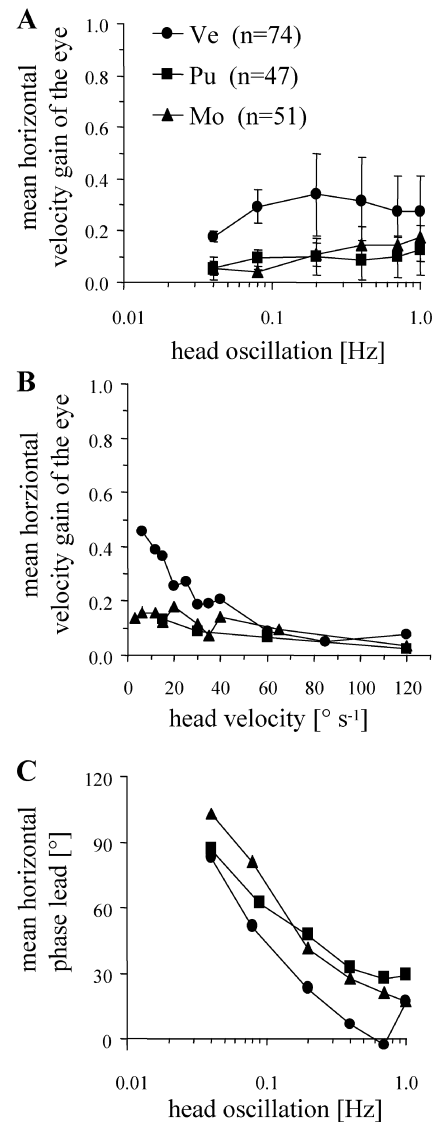


Fig. 1A–C Vestibular stimulation in the dark, head-fixed. **A** Mean horizontal gain (\pm SD) plotted against stimulation-frequency. **B** Mean horizontal gain plotted against peak stimulation-velocity. **C** Mean horizontal phase lead ($^\circ$) between stimulus and response signal plotted against stimulation frequency. Each data point represents the mean of all measurements in a particular stimulation condition; n = number of recordings (each of duration around 60 s) per animal over all stimulation conditions. Values for mean gains of each animal in Table 2

decreased with higher stimulation velocities (Fig. 2B), as seen during stimulation in the dark.

We found a phase lead of 30 – 0° , with lower values over the whole frequency-range than during stimulation in the dark (Fig. 2C).

Head-free conditions

Since it is technically challenging to do head-free 3D recordings in chameleons, we could record substantial data sets only in two animals (Mo, Pu), and only for one animal (Mo) was it possible to probe a large number of

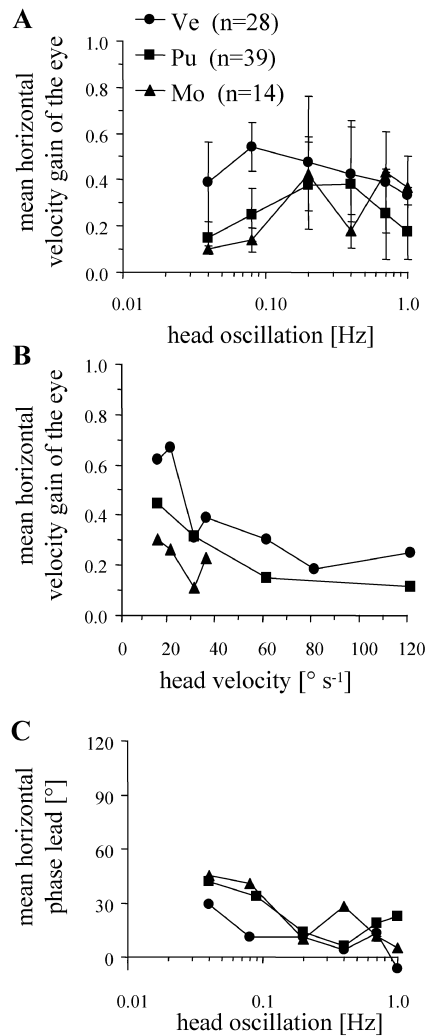


Fig. 2A–C Vestibular stimulation in the light, head-fixed. **A** Mean horizontal gain (\pm SD) plotted against stimulation-frequency. **B** Mean horizontal gain against peak stimulation-velocity. **C** Mean horizontal phase lead ($^{\circ}$) between stimulus- and response signal plotted against stimulation frequency. Same presentation as in Fig. 1

experimental conditions. However, the data obtained from both animals were similar in the overlapping part, as shown in Table 2.

During combined eye and head movements, the eyes exhibited slow phase and single superimposed saccadic movements with respect to the head, whereas the head generally moved smoothly with rare interjectional saccade-like movements. A 20-s extract of a raw data file during head-free stimulation in the light is given in Fig. 3, showing eye, head and turntable (i.e., stimulus) signal plotted against time. Superimposed on the sinusoidal curve of the eye velocity are a few spike-like elements, corresponding saccadic movements, which are not observed in the head velocity signal. Figure 3 illustrates the low head responses as compared to the gaze (and therefore the eye) response. During stimulation in the dark the gain of gaze, i.e., the sum of head and eye

Table 2 Mean gains per animal

Head-fixed stimulation	Gaze gain	Mean	SD	<i>n</i>
Vestibular (dark) (Fig. 1)	Ve	0.25	0.11	74
	Pu	0.09	0.03	47
	Mo	0.12	0.05	51
Vestibular (light) (Fig. 2)	Ve	0.41	0.14	28
	Pu	0.26	0.11	39
	Mo	0.25	0.13	14
Head-free stimulation	Gain	Mean	SD	<i>n</i>
Vestibular (dark) (Fig. 4)	Mo head	0.19	0.07	24
	Mo gaze	0.53	0.07	
Vestibular (light) (Fig. 5)	Mo head	0.42	0.06	23
	Mo gaze	0.78	0.08	
	Pu head	0.38	0.13	4
	Pu gaze	0.67	0.17	

gain, was around 0.5, slightly increasing from 0.4 to 0.6 with higher stimulation frequencies (Fig. 4). The head gain showed an increase from 0.1 at low stimulation frequencies to 0.25 for the 1-Hz stimulation. Therefore, the increase in gaze gain was due to increase in head gain. In contrast to the head fixed conditions, there was no dependence on stimulation velocity. We found a phase lead of about 30° over all stimulation frequencies for the gaze-signal.

Combined visual and vestibular stimulations delivered in head-free animals in the light resulted in a combination of VCR and opto-collic reflex (OCR), as well as VOR and optokinetic reflex (OKR). Gains of the gaze responses were around 0.8 (Fig. 5). For the combined visual and vestibular stimulation, we found similar dependencies between head- and gaze gain and stimulation frequency as for pure vestibular stimulation. In contrast to stimulation in the dark, values for head and gaze gain showed a slight decrease with higher stimulation velocities. There was nearly no phase difference between stimulation and gaze response.

Eye-position dependence of the VOR

To analyze the influence of eye position on VOR slow-phase axis orientation, tilt angles of rotation axes were computed using the 3×13 generalized gain matrix (see Materials and methods) and expressed for two vertically eccentric gaze directions: 20° up and 20° down from reference position. For the $20^{\circ} \text{ s}^{-1}$ stimulation condition we found relative tilt angles of the VOR slow phase rotation axis from -4.2 to 6.6° for 20° upward gaze and from -6.3 to 6.1° for 20° downward gaze. For the $40^{\circ} \text{ s}^{-1}$ stimulation condition a similar pattern was found with tilt angles ranging between -3.7 and 6.9° for upward gaze and -2.9 to 6.1° for downward gaze.

Figure 6 shows the values scattering along the z -axis with a relatively broad range of the gain represented by the value of the horizontal eye velocity and a smaller range of the eccentricity of the VOR rotation axes rep-

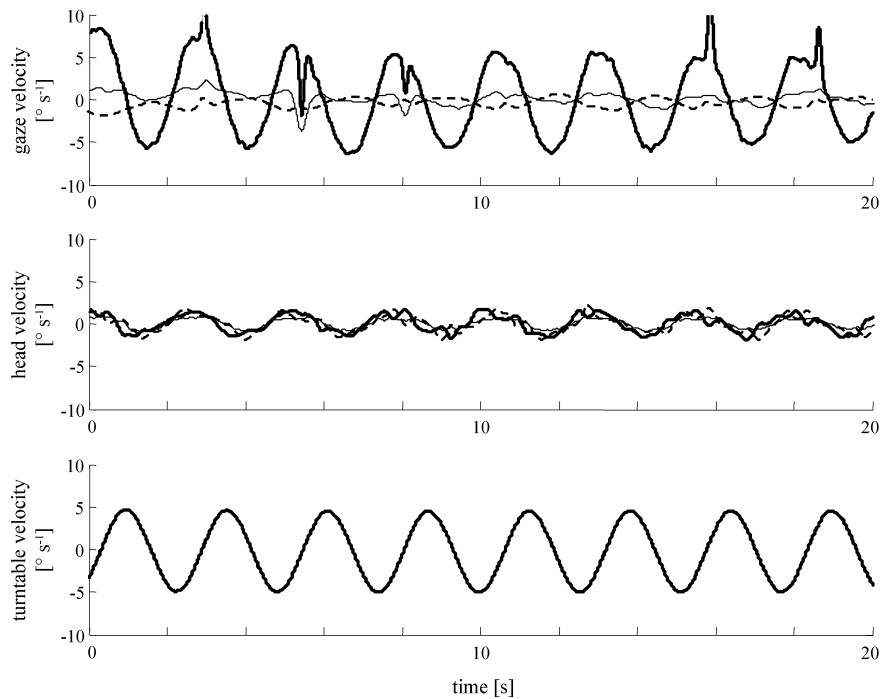


Fig. 3 Three-dimensional (3D) eye, head and turntable velocity during head-free vestibular stimulation in the dark. In the *upper panel*, eye velocity vectors ($^{\circ} \text{s}^{-1}$) are shown, in the *middle panel* the corresponding head velocity vectors are shown, and in the *bottom panel* turntable stimulation velocity is shown. The *thin line* represents the *x*-component (torsional), the *dashed line* is the *y*-component (vertical), and the *thick line* is the *z*-component (horizontal). Superimposed on the sinusoidal curve of the eye velocity are a few spike-like elements, corresponding to saccadic movements, which are not observed in the head velocity signal. As only relative information was needed from the head coil, no calibration was performed. In our example the head velocities seem to be similar in all three directions, which was only due to the way the coil was placed on the head

resented by the values on the *x*-axis (torsional eye velocity).

The results of our chameleon study show that, although the chameleon's saccadic eye movements obey LL (Sándor et al. 2001), chameleons follow, like monkeys, the VOR strategy of optimal retinal image stabilization with no influence of the orientation of gaze on VOR rotation axes.

Discussion

The main findings of our study are: (1) chameleon VOR has a low gain during head-restrained stimulation in the dark; (2) the gain increases during head-restrained stimulation in the light; and (3) the gain in gaze response obtained under vestibular and visual stimulation in the head-free condition is close to unity. These results confirm previous findings by Gioanni et al. (1993). Chameleon VOR is not affected by LL: eye position has no influence on VOR rotation axes.

Methodological considerations

In contrast to previous studies of chameleon gaze-stabilizing reflexes (Gioanni et al. 1993), which were performed by means of the single search coil technique, we used the dual search coil technique. In animals with an extremely large oculomotor range as the chameleons, a 2D system provides far less reliable information in the extremes of the oculomotor range and could eventually go into saturation. Furthermore, this technique enabled us to study 3D eye movements and allowed us to analyze the influence of eye position on VOR rotation axes.

Influence of the low gains on the analysis of position dependence: despite the finding that VOR gain is influenced by head restriction, head fixation was needed for calibration of the eye-in-head position, which was necessary to measure the effect of eye position dependence on the VOR. The calculations of the slow phase rotation axes orientation using the 3×3 generalized gain matrix are based on the rotation axis and not on the amount of VOR response. Therefore a decreased VOR gain did not influence this second part of our analysis.

Chameleon horizontal VOR characteristics: gain and phase

The characteristics of VOR gain show, that chameleons have a very low VOR gain during head-fixed conditions and stimulation in the dark and higher gains during head-free conditions and stimulation in the light. Quantitatively our results from one animal (Ve) are practically identical with the results of the previous study by Gioanni et al. (1993); the results from the other

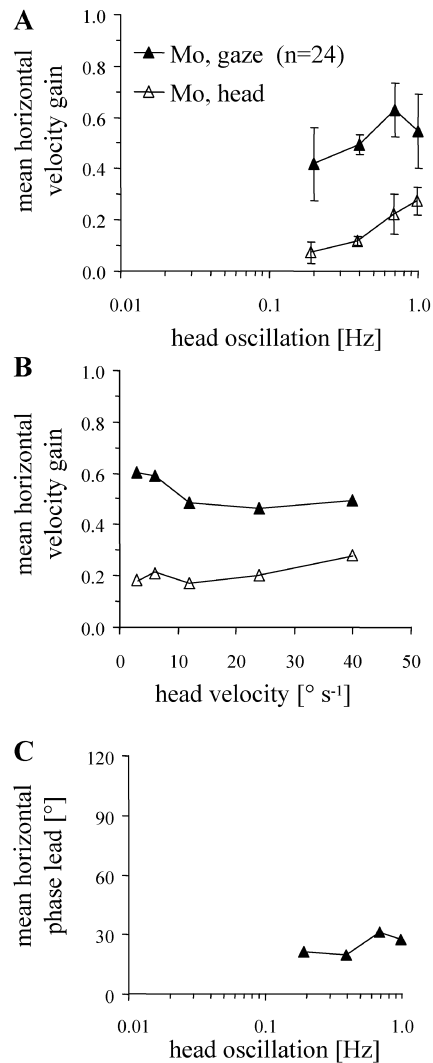


Fig. 4A–C Vestibular stimulation in the dark, head-free. **A** Mean horizontal gain (\pm SD) plotted against stimulation frequency. **B** Mean horizontal gain against peak stimulation velocity. *Filled symbols*: gaze gain (i.e., sum of head and eye gain). *Empty symbols*: head gain. **C** Mean horizontal phase lead ($^{\circ}$) between stimulus- and response (gaze) signal plotted against stimulation frequency. Same presentation as in Fig. 1

animals (Pu, Mo) were lower. Although the characteristics of the VOR were similar between all three animals, one of them (Ve) showed higher gains throughout all experimental conditions. This might be due to the fact that Ve was involved in numerous previous experiments and therefore was more habituated to the recordings. All three animals showed remarkably low gains under head-restrained conditions. These low values were probably due to the artificial situation of head restriction, since we observed a significant increase of gain in the chameleon Mo when measured unrestrained. The increase in gain under head-free conditions is a well-known phenomenon in primates and humans and may be due to an elevation of the threshold for motion detection that occurs during self motion (Probst et al. 1986). The visual image

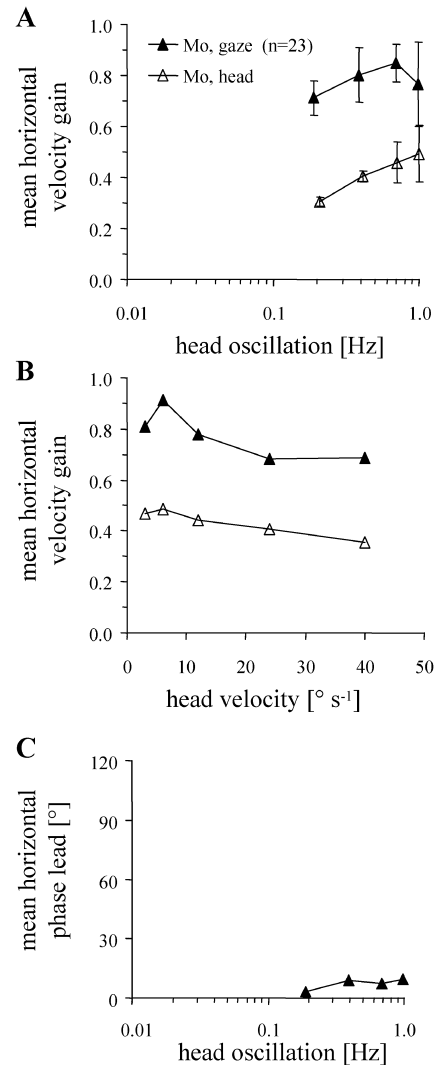


Fig. 5A–C Vestibular stimulation in the light, head-free. **A** Mean horizontal gain (\pm SD) plotted against stimulation frequency. *Filled symbols*: gaze gain (i.e., sum of head and eye gain). *Empty symbols*: head gain. **B** Mean horizontal gain against peak stimulation velocity. **C** Mean horizontal phase lead ($^{\circ}$) between stimulus- and response (gaze) signal plotted against stimulation frequency. Same presentation as in Fig. 1

stabilization was nearly optimal in experiments where the chameleons were allowed to move freely in an illuminated visual environment.

The small influence of stimulation frequency on VOR gain during head-fixed stimulation compared to the strong influence on VOR phase lead was also observed by Gioanni et al. (1993), as well as the increase in gain of head and gaze responses at higher frequencies during head-free stimulation. The fact that the phase lead of the gaze response is consistently lower during head-free experiments than under head-fixed conditions was observed in different species and has been attributed to the inertial properties of the head (Gioanni et al. 1993; humans: Outerbridge and Melville 1971; rabbits: Fuller 1981; pigeons: Gioanni 1988).

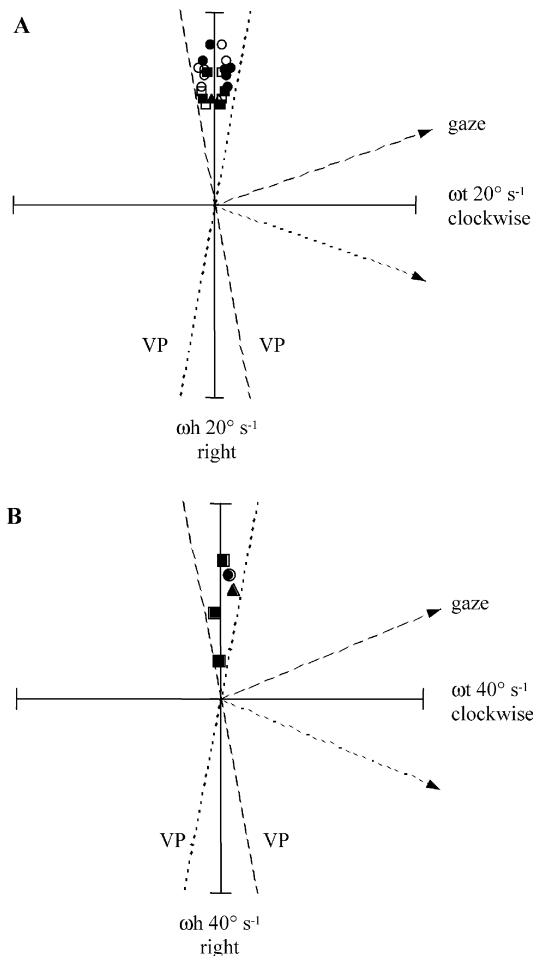


Fig. 6A, B Eye-position dependence of the vestibulo-ocular reflex (VOR). Each symbol in this figure represents the tip of an angular velocity vector of the eye seen from the chameleon's side. ω_t and ω_h are torsional and horizontal components of slow-phase eye velocity, respectively. The different symbols represent the data of the different animals (circles: Ve, squares: Pu, triangles: Mo). Empty symbols: 20° upward gaze; filled symbols: 20° downward gaze. **A** Head-fixed horizontal rotation in the light with 20° s⁻¹ peak stimulation velocity. **B** Same conditions with faster stimulation-velocity: 40° s⁻¹ peak stimulation velocity. Note that VOR eye rotation axes do not depend on eye position: In response to a rightward head rotation of 20° s⁻¹ (A), the tips of the slow phase eye velocity vectors lie close to the head's rotation axis (the ordinate), and do not obey the pattern predicted by Listing's law, i.e., axes do not lie along the dashed (for 20° up data: black empty symbols) or dotted (for 20° down data: black filled symbols) planes (labeled VP for velocity plane) when looking 20° up/down. **B** When the head rotates faster, 40° s⁻¹ rightward, the directions of VOR responses are almost identical, irrespective whether gaze is up or down.

The overall low VOR gains may also be due to the fact that the animal was not engaged in a behaviorally relevant task. We would expect a higher performance of visual image stabilization in the chameleon because of its arboreal lifestyle on undulating twigs, where externally induced motion has to be overcome for precise foveal fixation. In primates the VOR serves to compensate for movements of the head. Chameleons, however, tend to

sit motionless on branches for long periods of time. Therefore, it is sufficient if their stabilization reflexes compensate for whole-body movements due to externally induced motion, e.g., of a branch. One reason for using the VCR to solve such a problem is that it is not affected by either the magnitude of the oculomotor range or the amount of dependence between positions of the two eyes. This would strongly decrease the computations that have to be made in order to stabilize the retinal image in chameleons. However, retinal image stabilization depends not only on the gain of the VOR and OKR, but also on the orientation of its rotation axis, which, if optimal, has to be parallel to the rotation axis of the stimulus.

Chameleon horizontal VOR: eye position dependence

In the chameleon horizontal VOR, eye rotation axes roughly align with the (yaw) head rotation axis and do not systematically tilt in eccentric gaze directions as predicted by LL. This law of rotational kinematics, known to hold for the saccadic, fixational and smooth pursuit primate (e.g., Ferman et al. 1987; Minken et al. 1993; Tweed and Vilis 1990; Haslwanter et al. 1991; Tweed et al. 1992) and chameleon (Sándor et al. 2001) eye-movement systems, states that the axes of eye rotation lie in planes whose orientation depend on current eye position: when gaze direction changes by x° , then the planes containing the velocity vectors change by $x/2^\circ$ (half-angle rule, Helmholtz 1867; Tweed and Vilis 1990). This prediction is neither quantitatively nor qualitatively matched by our data: The obtained values scatter around zero and there is no systematic tilt. The small tilt coefficient values (mean: 0.20) show that the VOR of the chameleon is closer to an optimal VOR than to a VOR following LL.

Using a similar analysis as applied here, previous work showed a systematic dependence of VOR responses as a function of gaze direction in the human (Misslisch et al. 1994, 1996) but not in the monkey VOR (Misslisch and Hess 2000). With respect to the functional significance of the human VOR, Misslisch et al. (1994) pointed out that it stabilizes the foveal image, at the cost of image slip across the retinal periphery, while reducing deviations from LL. In rhesus monkeys, the VOR strategy is to stabilize the entire retinal image, rotating the eyes around an axis always parallel with the head's rotation axis (optimal VOR). Misslisch and Hess (2000) suggested that the differences in primate VOR function reflect differences in the organization of the visual system in human and non-human primates, with a greater emphasis on foveal vision in humans than in monkeys. This notion is supported by work that compared cortical magnification factors in humans and macaques (Serenio et al. 1995; Tolhurst and Ling 1988) but is challenged by subsequent studies (Horton and Hocking 1997; Serenio 1998).

Although the visual angle of the chameleon is around 100° (Ott and Schaeffel 1995), retinal ganglia cells of the accessory visual system, responsible for the VOR, project evenly over the entire retina (Bellintani and Ott 2002). Which means, that the entire retina is sensitive to movements of the visual field. This is consistent with our finding, that chameleon's VOR responses follow, similar to monkeys, a stabilization also of peripheral retinal areas, which is in contrast to the above-described greater emphasis on foveal vision in humans. This is compatible with the observation that during our experiments the animals scanned their environment using saccadic, separate eye movements without any fixed orientation of the eyes with respect to each other (Frens et al. 1998). It is also known that during fixations directly preceding prey catching, chameleons change their oculomotor behavior and use binocular fixation (Flanders 1985; Ott 2001). Therefore, it would be of interest to study oculomotor behavior in these situations during vestibular stimulation using binocular 3D techniques.

Acknowledgements H.H. would like to express her gratitude to Volker Henn, who initiated this project a few months before he died. Many thanks to Jan Cabungcal, Hansjörg Scherberger, Simon Elsaesser and Bernhard Hess. We would like to thank Paul Hofman, University of Nijmegen, for his permission to use his desaccading program Megadet. Animal housing and experiments were carried out in accordance with the regulations of the Veterinary Office of the Canton of Zurich, the European Communities Council Directive of 24 November 1986 (86/609/EEC), and guidelines of the Animal Welfare Committee of the University Hospital of Zürich.

References

- Bellintani-Guardia B, Ott M (2002) Displaced retinal ganglion cells project to the accessory optic system in the chameleon (*Chamaeleo calyptratus*). *Exp Brain Res* 145:56–63
- Ferman L, Collewyn H, Van den Berg AV (1987) A direct test of Listing's law. I. Human ocular torsion measured in static tertiary positions. *Vision Res* 27:929–938
- Flanders M (1985) Visually guided head movement in the African chameleon. *Vision Res* 25:935–942
- Frens M, Hepp K, Suzuki Y, Henn V (1996) Rotational kinematics and eye position dependence during vestibular-optokinetic stimulation in the monkey. *Ann N Y Acad Sci* 781:622–624
- Fuller JH (1981) Eye and head movements during vestibular stimulation in the alert rabbit. *Brain Res* 205:363–381
- Gioanni H (1988) Stabilizing gaze reflexes in the pigeon. II. Vestibulo-ocular (VOR) and vestibulo-colic (closed-loop VCR) reflexes. *Exp Brain Res* 69:583–593
- Gioanni H, Bennis M, Sansonetti A (1993) Visual and vestibular reflexes that stabilize gaze in the chameleon. *Vis Neurosci* 10:947–956
- Haslwanter T, Straumann D, Hepp K, Hess BJ, Henn V (1991) Smooth pursuit eye movements obey Listing's law in the monkey. *Exp Brain Res* 87:470–472
- Haustein W (1989) Considerations on Listing's Law and the primary position by means of a matrix description of eye position control. *Biol Cybern* 60:411–420
- Helmholtz HLF (1867) *Handbuch der physiologischen Optik*. Voss, Hamburg, Germany
- Horton JC, Hocking DR (1997) Relative magnification of the central visual field representation in striate cortex of macaques and humans. *Soc Neurosci Abstr* 23:1945
- Kirmse W (1988) Foveal and ambient visuomotor control in chameleons. *Zool Jahrb Abt Allg Zool Physiol* 92:341–350
- Minken AW, Van Opstal AJ, Van Gisbergen JA (1993) Three-dimensional analysis of strongly curved saccades elicited by double-step stimuli. *Exp Brain Res* 93:521–533
- Misslisch H, Hess BJ (2000) Three-dimensional vestibulo-ocular reflex of the monkey: optimal retinal image stabilization versus Listing's law. *J Neurophysiol* 83:3264–3276
- Misslisch H, Tweed D, Fetter D, Sievering D, Koenig E (1994) Rotational kinematics of the human vestibulo-ocular reflex. III. Listing's law. *J Neurophysiol* 72:2490–2502
- Misslisch H, Tweed D, Fetter M, Dichgans J, Vilis T (1996) Interaction of smooth pursuit and the vestibulo-ocular reflex in three dimensions. *J Neurophysiol* 75:2520–2530
- Ott M (1997) *Visuelle Zielpeilung, Akkomodation und funktioneller Bau des Auges beim Chamäleon*. Dissertation (PhD), Fakultät für Biologie der Eberhard-Karls-Universität Tübingen
- Ott M (2001) Chameleons have independent eye movements but synchronise both eyes during saccadic prey tracking. *Exp Brain Res* 139:173–179
- Ott M, Schaeffel F (1995) A negatively powered lens in the chameleon. *Nature* 373:692–694
- Outerbridge JS, Melvill J (1971) Reflex vestibular control of head movement in man. *Aerosp Med* 42:935–940
- Palla A, Straumann D, Obzina H (1999) Eye-position dependence of three-dimensional ocular rotation-axis orientation during head impulses in humans. *Exp Brain Res* 129:127–133
- Pettigrew JD, Collin SP, Ott M (1999) Convergence of specialised behaviour, eye movements and visual optics in the sandlance (Teleostei) and the chameleon (Reptilia). *Curr Biol* 9:421–424
- Probst T, Brand T, Degner D (1986) Object-motion detection affected by concurrent self-motion perception: psychophysics of a new phenomenon. *Behav Brain Res* 22:1–11
- Sándor PS, Frens M, Henn V (2001) Chameleon eye position obeys Listing's law. *Vision Res* 41:2245–2251
- Sereno MI (1998) Brain mapping in animals and humans. *Curr Opin Neurobiol* 8:188–194
- Sereno MI, Dale AM, Reppas JB, Kwong KK, Belliveau JW, Brady TJ, Rosen BR, Tootell RB (1995) Borders of multiple visual areas in humans revealed by functional magnetic resonance imaging. *Science* 268:889–893
- Solomon D, Straumann D, Zee DS (1997) Three-dimensional eye movements during vertical axis rotation: effects of visual suppression, orbital eye position and head position. In: Fetter M, et al (eds) *Three-dimensional kinematic principles of eye, head and limb movements*. Harwood, Chur, Switzerland, pp 197–208
- Straumann D, Zee DS, Solomon D, Lasker AG, Roberts DC (1995) Transient torsion during and after saccades. *Vision Res* 35:3321–3334
- Tauber ES, Atkin A (1967) Disconjugate eye movement patterns during optokinetic stimulation of the African chameleon, *Chamaeleo melleri*. *Nature* 214:1009–1010
- Tolhurst DJ, Ling L (1988) Magnification factors and the organization of the human striate cortex. *Hum Neurobiol* 6:247–254
- Tweed D, Vilis T (1990) Geometric relations of eye position and velocity vectors during saccades. *Vision Res* 30:111–127
- Tweed D, FM, Andreadaki S, Koenig E, Dichgans J (1992) Three-dimensional properties of human pursuit eye movements. *Vision Res* 32:1225–1238
- Tweed D, Sievering D, Misslisch H, Fetter M, Zee D, Koenig E (1994a) Rotational kinematics of the human vestibulo-ocular reflex. I. Gain matrices. *J Neurophysiol* 72:2467–2479
- Tweed D, Fetter M, Sievering D, Misslisch H, Koenig E (1994b) Rotational kinematics of the human vestibulo-ocular reflex. II. Velocity steps. *J Neurophysiol* 72:2480–2489